Pharm Res (2012) 29:187–197
DOI 10.1007/s11095-011-0534-2

RESEARCH PAPER

Characterization of the Isomerization Products of Aspartate Residues at Two Different Sites in a Monoclonal Antibody

Alavattam Sreedhara • Armando Cordoba • Qing Zhu • Jeanne Kwong • Jun Liu

Received: 24 March 2011 / Accepted: 7 July 2011 / Published online: 2 August 2011
© Springer Science+Business Media, LLC 2011

ABSTRACT

Purpose To identify and understand isomerization products and degradation profile of different aspartate residues in an IgG1 monoclonal antibody.

Methods Recombinant IgG1 was incubated for extended periods of time in a formulation buffer at recommended and accelerated storage temperatures. Isomerization reaction products were analyzed using ion exchange chromatography (IEC), hydrophobic interaction chromatography (HIC), peptide mapping, and LC-MS. Model peptides with sequences containing specific aspartate residues in IgG1 were synthesized and incubated under accelerated conditions. Products of isomerization reactions of peptides were analyzed by reverse phase chromatography (RP-HPLC) and LC-MS. X-ray crystallography data from Fab of IgG1 were used to understand mechanism of isomerization reactions.

Results A MAb containing labile Asp32-Gly sequence in CDR I region undergoes rapid isomerization reaction and leads to formation of isoaspartate (IsoAsp) and cyclic imide (Asu) forms. Isomerization of aspartate residues was observed in a non-CDR region containing Asp74-Ser sequence. Isomerization reaction at Asp74-Ser led to formation of Asu74 and trace isoAsp74. While isoAsp32 increased linearly with time, isoAsp74 did not increase during storage. Asu32 and Asu74 followed non-linear degradation kinetics and reached steady state over time. Isomerization reaction of two different model peptides containing Asp32-Gly or Asp74-Ser with neighboring amino acid sequences as those found in the MAb result in formation of IsoAsp.

Conclusions Observed levels of Asu and trace IsoAsp at the Asp74 site are unusual for typical isomerization reactions. In addition to primary sequences, pKa, solvent exposure and high order structure around aspartate residues may have influenced isomerization reaction at Asp74 in MAbI. Different degradation profiles from the two Asp residues can influence shelf life and should be carefully evaluated during product development.

KEY WORDS aspartic acid · higher order structure · isomerization · monoclonal antibodies · shelf-life

INTRODUCTION

Proteins are highly sensitive Active Pharmaceutical Ingredients (API) that are susceptible to both chemical and physical degradation during storage and delivery. Proteins, including monoclonal antibodies (MAbs), undergo chemical degradation via several different mechanisms that include oxidation, deamidation, isomerization, and fragmentation, amongst other reactions resulting in the formation of

Alavattam Sreedhara and Armando Cordoba contributed equally.

A. Sreedhara (✉) · Q. Zhu · J. Liu
Late Stage Pharmaceutical Development
Genentech, Inc.
1 DNA Way
South San Francisco, California 94080, USA
e-mail: sreedhaa@gene.com

A. Cordoba · J. Kwong
Protein Analytical Chemistry,
Genentech, Inc.
1 DNA Way
South San Francisco,
California 94080, USA

various charge variants and heterogeneity (1–4). Due to the potential influence on stability and biological activity, these variants need to be fully evaluated and characterized. Appropriate testing and control may be needed to ensure the quality of the product. Asparagine (Asn) deamidation and Aspartic acid (Asp) isomerization are the most ubiquitous covalent modifications that result in charge heterogeneity in MAbs (5) and are typically regarded as one of the major indicators for the chemical stability during protein pharmaceutical development. Asp isomerization in many MAbs leads to formation of isoaspartate (IsoAsp) via the cyclic imide (Asu) pathway (Scheme 1). However, the formation of isoAsp is not always detected due to analytical or conformational constraint (6). The isomerization reaction can cause significant physicochemical and functional changes to the protein, and hence it is imperative to accurately monitor and control the isomerization variants. Several analytical methods have been developed over the past years to study the isomerization reactions and their intermediates with reasonable precision and accuracy (7–9). Wakankar and Borchardt have reviewed the influence of formulation conditions, protein primary sequence, solvent dielectric, pH, and protein structure on the reactivity of Asn and Asp residues in proteins (10). The effects of various amino acids at the C-terminal position adjacent to the Asp residue have been studied extensively, indicating that C-terminal glycine and serine facilitate the Asp isomerization reaction in several model peptides and proteins (11–14), whereas histidine residue has been identified to be particularly influential when it was found at the N-terminus of the Asp residue (15). Apart from the isomerization reaction, aspartic acid residues are known to undergo hydrolysis reactions, and several mechanisms for the aspartyl peptide hydrolysis have been proposed (4,15, 16). Oliyai and Borchardt have previously reported that the Asp-Gly undergoes amide bond hydrolysis under very acidic pH values (0.3–3.0), while at pH≥6 only isomerization to isoAsp was noticed (16).

A previous study showed that aspartic acid residues on the complementarity determining regions (CDRs) of two closely related MAbs (MAbI and MAbII) were highly prone to isomerization reactions at different rates (17). The isomerization of Asp32 in MAbI led to significant reduction of binding affinity. The differences in the Asp isomerization rates between MAbI and MAbII has been attributed to structural factors and solvent exposure of the Asp residues in these antibodies (17). Extensive analytical characterization of MAbs, including the isomerization reaction and product characterization, effect of protein structure on deamidation, isomerization and succinimide hydrolysis, have been reported in the literature (18–22). Recently, the thermodynamic and kinetic controls on the Asn deamidation and Asp isomerization, as well as the comparative kinetic rates of model peptides and monoclonal antibodies, have also been discussed (23,24). Interestingly, studies on the isomerization reactions of MAbI and MAbII and also the model peptide from the primary sequences of these mAbs indicate that isomerization rates of Asp32 in MAbI were faster than the corresponding peptide at pH>6.0, suggesting a potential catalytic effect due to secondary or tertiary structural features found in MAbI (17). In addition to Asp32, we report here that Asp74 in MAbI also undergoes significant isomerization reaction under normal storage condition of 2–8°C. While Asp74 is located outside the CDR regions, the rate of its degradation, in addition to the isomerization reaction at Asp32, is also significant, as it may affect the product shelf life. To understand the mechanism of Asp74 isomerization, and to figure out if the mechanism was similar to that of Asp32, small model peptides containing neighboring amino acid residues around Asp74 were prepared and Asp isomerization reactions were studied and compared with that in a full length MAb.

The stability of MAbI under normal and accelerated conditions was monitored by using two stability-indicating chromatography methods. A hydrophobic interaction chromatography (HIC) method was used to monitor the isomerization products of Asp32, while an ion exchange chromatographic method was used to monitor the Asu32 and Asu74 formation. These results have been used to better understand the degradation mechanism of aspartate in a monoclonal antibody.

MATERIALS AND METHODS

Materials

A humanized monoclonal antibody, MAbI, was expressed in Chinese hamster ovary (CHO) cell lines and purified by a series of chromatography methods including affinity purification by protein A chromatography and ion-exchange chromatography. The antibody was formulated as a liquid product in 20 mM histidine, 200 mM arginine HCl, 0.04% polysorbate 20 at pH 6.0 using TFF process. All the chemical reagents were analytical grade or higher. Papain and anti-papain (Antipain) were purchased from Roche Diagnostics (Mannheim, Germany) and Peptide International (Louisville, KY), respectively. Water used in these experiments was purified using Millipore MILLI-Q system.

Model peptides corresponding to the neighboring sequence of Asp74 site in the MAbI were synthesized and purified at Genentech. The ISRDDSK peptides and

Scheme 1 Typical pathway of Asp isomerization in proteins and peptides (21).

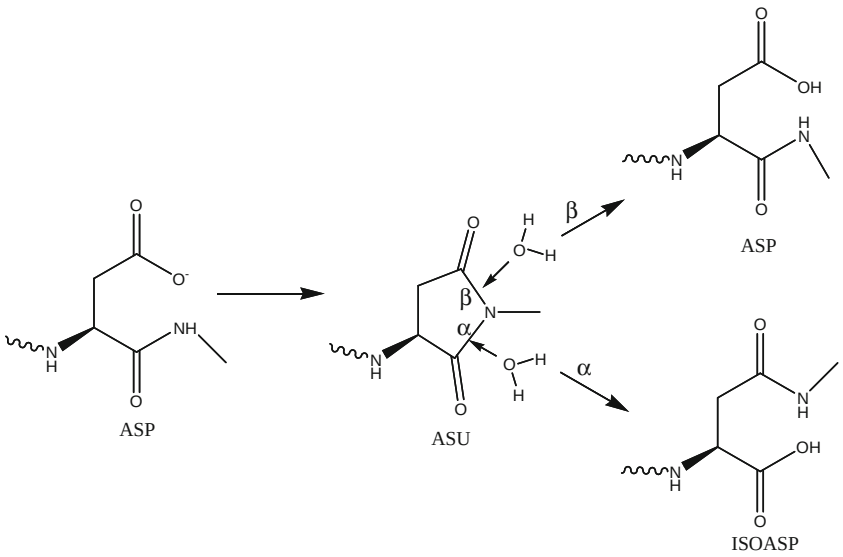

derivatives ISRdDSK and ISRDdSK had their N-termini acetylated and their C-termini amidated, while the GRITISRDDSK and its derivatives GRITISRdDSK and GRITISRDdSK peptides (wherein d is iso-Asp) had a free amino and a free carboxyl terminal.

MATERIALS AND METHODS

Ion Exchange Chromatography (IEC) of Carboxypeptidase B (CpB) Digested MAbI

IEC is used to measure the charge variants of MAbI. Partial removal of C-terminal lysines from the heavy chain is a common cause of charge heterogeneity in monoclonal antibodies. These lysine residues are typically removed by treating the MAb with carboxypeptidase B (CpB). Samples were diluted to 1 mg/mL with a buffer containing 20 mM MES (2-[N-Morpholino] ethanesulfonic acid), pH 6.1 and then treated with carboxypeptidase B (CpB, DFP treated, Roche) at a 1:100 (w:w) ratio. The samples were incubated at 37°C for 20 min prior to ion exchange analysis. A Dionex ProPac Weak Cation Exchange (WCX) column (4×250 mm) was equilibrated at 0.8 mL/minute and 48°C with 50% solvent A (20 mM MES, pH 6.1) and 50% solvent B (solvent A containing 100 mM sodium chloride). Following injection of approximately 50 μg of CpB-treated MAbI, a linear gradient increasing from 50% to 80% solvent B in 50 min, then from 80% to 100% solvent B in 10 min, was initiated. The column was regenerated by washing at 100% of solvent B for 5 min, then re-equilibrated with 50% solvent B for 20 min. Chromatography was carried out using an Agilent 1100 HPLC instrument. The column effluent was monitored at 280 nm and 214 nm.

Semi-preparative Ion Exchange Chromatography (IEC) of Carboxy-peptidase B (CpB) Digested MAbI

Semi-preparative IEC was used to collect peak fractions with various charge variants for further characterization. MAbI samples were diluted to 10 mg/mL with a buffer containing 20 mM MES, pH 6.1 and then treated with carboxypeptidase B (CpB, DFP treated, Roche) at a 1:100 (w:w) ratio. The column used was a semi-prep Dionex ProPac Weak Cation Exchange (WCX) (9× 250 mm), equilibrated at 3 mL/min and 48°C with 50% solvent A (20 mM MES, pH 6.1) and 50% solvent B (solvent A containing 100 mM sodium chloride). Following injection of approximately 2.5 mg of CpB-treated MAbI, a linear gradient increasing from 50% to 57% in 1 min, 57% to 80% solvent B in 38 min, and from 80% to 100% solvent B in 10 min, was initiated. The column was regenerated by washing at 100% of solvent B for 2 min, then re-equilibrated with 50% solvent B for 20 min. Chromatography was carried out using an Agilent 1100 HPLC instrument. The column effluent was monitored at 280 nm and 214 nm. Peak fractions (main peak and basic peak 2) were collected from multiple injections for analysis by papain digestion with hydrophobic interaction chromatography (HIC), IEC, Lys-C peptide mapping, or by ESI-MS, using procedures described below. Fractions were collected using an Agilent 1100 series Analytical Fraction Collector using time-based peak collection. Each collected fraction was then pooled, concentrated and exchanged into 20 mM Tris, pH 7.4, using Amicon Ultra-15, 30,000 MWCO centrifugal filter devices (Millipore). After concentration, fractions were tested for purity by running them in the IEC method described above.

Hydrophobic Interaction Chromatography (HIC) of Papain Digested MAbI

HIC was used to monitor the isomerization products of MAbI. Selective protease (papain or pepsin) digestion followed by separation of the fragments has been employed to characterize the source of heterogeneity in MAb (9). Papain digestion followed by HIC analysis was instrumental in characterizing Asp isomerization for MAbI and has since been used routinely (9). MAbI samples were diluted to 1 mg/mL in a solution containing 0.1 M Tris-HCl, 4 mM EDTA, 1 mM cysteine, pH 7.4. Papain was added at a 1:100 (w:w) enzyme:substrate ratio and incubated for 2 h at 37°C. The resulting digest was analyzed on a TSK Phenyl 5PW column (7.5×75 mm) using an 1100 Agilent HPLC system. The column was equilibrated with 75% of solvent A containing 2 M ammonium sulfate solution, 20 mM Tris-HCl, pH 7.5 and 25% solvent B containing 20 mM Tris-HCl, pH 7.5. The column temperature was 40°C and flow rate was 1 mL/min. Following injection of about 30 µg of papain-digested MAbI, solvent B remained at 25% for 1 min, then a two-step linear gradient proceeded from 25% to 40% solvent B in 3 min and then from 40% to 80% solvent B in 40 min. Solvent B was then increased to 100% for 2 min to regenerate the column, followed by re-equilibration at 25% solvent B. The column effluent was monitored at 214 nm.

Peptide Map Analysis Using Lys-C Enzyme

The method involves disrupting the secondary structure of the protein by sulfitolysis followed by digestion with Lys-C at an enzyme to substrate ratio of 1:75 (w:w) for 5 h at 37°C. The resulting peptides are resolved by RP-HPLC on an Agilent 1100 HPLC system with a ZORBAX 300SB-C8 column at 44°C with a flow rate of 0.5 mL/min. The Lys-C peptides were separated using a linear gradient from 0% solvent B to 31% solvent B in 124 min after a 5-min hold at initial conditions, then to 95% solvent B at 146 min. Solvent A is 0.1% trifluoroacetic acid (TFA), while solvent B is 0.08% TFA in isopropyl alcohol. The column is washed with 95% solvent B and re-equilibrated to 100% solvent A before the next sample. The sample injected was approximately 50 µg.

For the peptide mapping analysis of the IEC fractions, S-carboxymethlylation of the fractions was performed prior to digestion with Lys-C. Samples were diluted to 1 mg/ml in a buffer containing 6 M guanidine, 0.36 M Tris, 3 mM EDTA at pH 8.6. Dithiothreitol (DTT) was added to bring the samples to 10 mM DTT, and the samples were then incubated at 37°C for 1 h. Iodoacetic acid was then added to a concentration of 35 mM. Samples were incubated for 20 min at ambient temperature in the dark. The alkylation was quenched by adding DTT to a final concentration of 30 mM. The reduced and S-carboxymethylated samples were exchanged using NAP-5 columns and eluted with 10 mM Tris, 100 mM NaOAc, 0.1 mM CaCl2, pH 8.0. Lys-C (Roche) was added to the samples at 1:75 Lys-C: sample (w/w). Digestion was allowed to proceed for 5 h at 37°C. Chromatographic conditions were the same as described in the previous paragraph. The sample injected was approximately 50 µg. For LC-ESI-MS of the peptide digests, the effluent from the HPLC was directed into a fused silica capillary to a Thermo Fisher LTQ XL linear ion trap mass spectrometer (San Jose, CA, USA) operating in positive ion mode. Mass data were analyzed using Thermo Scientific Xcalibur software.

ESI-MS Analysis of IEC Fractions

A liquid chromatography-mass spectrometry (LC-MS) system was used for MS analysis of the IEC fractions. Samples (1–2 µg) were loaded onto a Poros R1 column (0.33×200 mm) that had been equilibrated at 0.5 mL/minute with 0.1% formic acid (solvent A) at a column temperature of 70°C. Samples were separated using a linear gradient from 25% solvent B (0.2% formic acid in acetonitrile) to 70% solvent B in 16 min. The eluent was directed to a PE Sciex API 3000 electrospray ionization triple quadrupole mass spectrometer operating in the positive ion mode. The electrospray voltage was 5 kV with an orifice potential of 80 V. For analysis after reduction, samples were incubated in 25 mM DTT for 30 min at 37°C prior to LC-MS analysis. LC-MS data were interpreted using the PE Sciex BioAnalyst 1.4 deconvolution software program, with masses determined by converting a series of multiply charged ion peaks into distinct molecular mass peaks.

RP-HPLC Analysis of Peptides

The parent peptides and their degradation products were separated using an Agilent Zorbax 300SB-C18, 5 um, 2.1×150 mm column at 30°C with a flow rate of 0.25 ml/min. The peptides were separated using a linear gradient from 0% solvent B to 11% solvent B in 40 min. Solvent A is 0.1% trifluoroacetic acid (TFA), while solvent B is 0.08% TFA in acetonitrile. The column is washed with 80% solvent B for 4 min and re-equilibrated to 100% solvent A before the next sample. The sample injected was approximately 10 µg.

RP-HPLC was performed using an Agilent 1100 HPLC system, which included a UV detector set at 214 nm for quantification. The degradation products were identified based on mass spectrometry (MS) analysis.

For MS analysis, a linear ion-trap (LTQ XL) mass spectrometer equipped with electron transfer dissociation (ETD) source (Thermo Fisher Scientific, San Jose, CA) was operated in a positive ionization mode with spray voltage and capillary temperature of 4.5 kV and 300°C, respectively. In ETD experiments, multiply charged parent ions were isolated in a linear trap with a 3 amu isolation window and subjected to an ion/ion reaction with radical anions of fluoranthene for 115 ms. Ion/ion reaction was accompanied by supplemental collisional activation at resonant frequencies of charge-reduced species. ETD was performed on doubly charged precursor ions during chromatographic separation of peptides of interest.

Stability Studies

Several lots of MAbI at 150 mg/mL in 20 mM histidine, 200 mM arginine HCl, 0.04% polysorbate 20 at pH 6.0 were stored at 2–8°C for more than 2 years. One mL of these solutions were filled in 3 cc glass vials, which were then sealed and capped. The stability of drug products was measured using IEC and HIC. IEC and HIC were identified as the shelf-life-limiting assays; therefore, the result from these assays were used to project the shelf life of drug product. The stability of product at the elevated temperature of 25°C was also evaluated to elucidate the major degradation products and the mechanism of these degradations.

Similarly, 1 mL of model peptide formulations at 1.0 mg/mL containing 20 mM histidine, 200 mM arginine HCl, 0.04% polysorbate 20 at pH 6.0 were stored in 3 cc glass vials or eppendorf tubes at 25°C and/or 40°C. Samples were tested at different time points using RP-HPLC to monitor loss of parent peptides and the formation of isoAsp and succinimide forms.

RESULTS AND DISCUSSION

Asp Isomerization in MAbI by HIC and IEC Analysis

The analysis of Asp isomerization at the CDR1 of the light chain Asp32 and at the heavy chain Asp74 in MAbI was conducted using the HIC and IEC assays described above. Figure 1 shows the HIC elution profile of a papain-digested MAbI sample. The resulting Fab peaks were previously identified by a combination of analytical methods including mass spectrometry, peptide map and N-terminal sequence analyses. The major degradation products, Fab peaks 3 and 5, were identified as isoAsp32 and Asu32, respectively, and peak 2 contains Asp32 and free thiol group (18).

Figure 2 shows the IEC elution profile of MAbI. Assignment of the characteristics that distinguish these peaks is challenging due to the combination of potential species caused by the symmetric nature of the molecule consisting of two identical heavy and light chains. Peak fractions were previously assigned by a combination of methods, including HIC after papain digestion, ESI-MS with and without prior reduction, tryptic peptide mapping, hydroxylamine cleavage and protein sequence analysis (18).

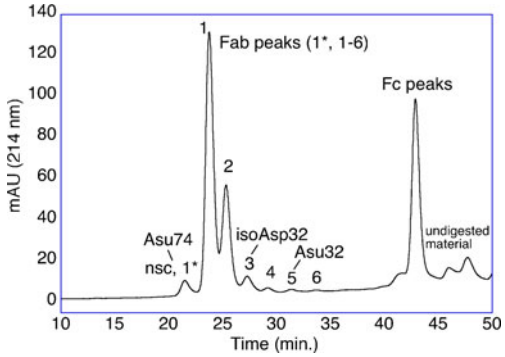

Fig. 1 HIC elution profile of a papain digested MAbI sample. Peak 1* corresponds to Asu74; nsc = non-specific clip due to papain cleavage, coelutes with peak 1*; Peak 2 is Asp32 with a free thiol group; Peak 3 corresponds to isoAsp32; and Peak 5 corresponds to Asu32.

ESI-MS analysis of IEC basic peaks 1 and 2 showed a minor form of the light chain and the heavy chain (respectively) with a mass difference of approximately 18 Da, consistent with the presence of a succinimide in this region. Specifically, IEC basic peak 2 was further identified previously to be Asu74 by collecting the peak, digesting it with papain and analyzing by HIC (18). The resulting increasing HIC peak 1* (Fig. 1) was again collected, and incubated in hydroxylamine prior to N-terminal sequence analysis. N-terminal sequence analysis of HIC peak 1* showed a clip between heavy chain Asp74 and Ser75, consistent with the presence of a succinimide at

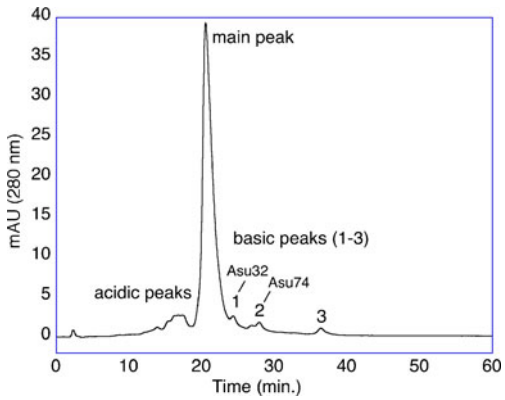

Fig. 2 Representative ion exchange chromatogram (IEC) of MAbI. Acidic peaks consist of deamidation in HC: 375–396 peptide and sialic acid derivatives. Basic peak 1 corresponds to LC:Asu32/Asp32, or HC:Met(O) 432/Met432; Basic Peak 2 corresponds to Val-His-Ser on one light chain, or HC:Asu74/Asp74 and Basic Peak 3 corresponds to Val-His-Ser extension on one heavy chain.

heavy chain Asp74. The relatively more basic elution position of IEC basic peak 2 is expected due to the loss of a carboxyl group on the side chain after succinimide formation. Similarly, papain digestion/HIC of IEC basic peak 1 resulted in an increase in HIC peak 5 (Asu32, described above) and was assigned as light chain Asu32 in the same way as IEC basic peak 2. All peaks in the IEC assay had similar activity to the main peak, indicating that the presence of a succinimide in one heavy chain or one light chain does not significantly affect the activity of full length MAbI (18).

Evaluation of IsoAsp 74

A summary of the detection of the isomerization products of MAbI by HIC and IEC is shown in Table 1. As isoAsp74 was not detected by HIC or IEC (Table 1); additional studies were conducted to determine if this is due to the lack of IsoAsp74 or because of an assay limitation. The Asu74 peak (basic peak 2 from IEC) was collected by preparative IEC after CpB digestion and then hydrolyzed by different pH and temperature conditions to convert the succinimide to Asp/isoAsp products for further characterization. The collected IEC basic peak 2 fractions were pooled and buffer exchanged into stock solution in formulation buffer containing 20 mM histidine, 200 mM arginine HCl, 0.04% polysorbate 20 at pH 6.0 (Asu74-T0). A similar procedure was also conducted with main peak fraction. The resulting IEC basic peak 2 pool was then divided into various aliquots and buffer exchanged into 1) 20 mM His, 133 mM NaCl, pH 5.5; 2) 20 mM NaH2PO4, 106 mM NaCl, pH 7.0; 3) 20 mM NaH2PO4, 92 mM NaCl, pH 8.0. The Asu74-T0 sample was kept frozen until further analysis; all the other samples at the different pHs were incubated overnight at 37°C. The Asu74-T0 sample, the pH-treated Asu74 fractions, and the IEC main peak fraction were then analyzed by IEC, HIC and Lys-C peptide maps, as described below.

Cation exchange (IEC) profiles for the IEC main peak and Asu74 fractions are shown in Fig. 3. The Asu74-T0 fraction contains 87% of Asu74 (Basic peak 2) with trace amounts of IEC main peak (believed to be due to succinimide instability). As expected, Asu74 hydrolyzed faster at pH 7 and 8, resulting in an increase in the IEC main peak which contains Asp and/or isoAsp. However, no new peak or noticeable increase in other peaks was detected from the hydrolysis of the Asu74 fractions, indicating that isoAsp74, if present, would coelute with the main peak in IEC.

Table 1 Isomerization Products of MAbI

Form	HIC (Fab peaks)	IEC (Full length MAb)
Asp32	peak 1	main peak
Asp74	peak 1	main peak
isoAsp32	peak 3	co-elutes with main peak
isoAsp74	not detected	not detected
Asu32	peak 5	basic peak 1
Asu74	peak 1* (with co-eluting peak)	basic peak 2

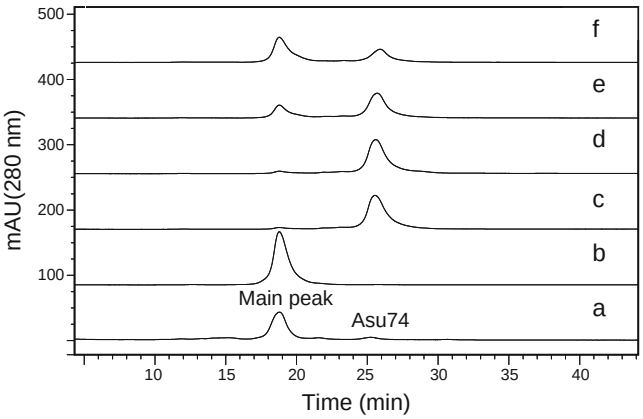

Fig. 3 Cation Exchange (IEC) profiles of aged MAbI and IEC Asu74 fractions. (**a**) Aged MAbI (t = 3 years @ 5°C + 23 days at 25°C); (**b**) IEC Main Peak; (**c**) Asu74-T0; (**d**) Asu74, pH 5.5; (**e**) Asu74, pH 7.0; (**f**) Asu74, pH 8.0.

Papain/HIC profiles for the IEC main peak and Asu 74 fractions are given in Fig. 4. The IEC Asu74-T0 fraction generates the highest levels of HIC peak 1* (Asu74 Fab form, which co-elutes with the non-specific clip peak). An increase in peak 3 (isoAsp32) was also observed. As expected, samples that were incubated at the higher pH showed a decrease in the HIC Asu74 peak compared to the lower pH fractions, due to the hydrolysis of Asu74 to Asp/isoAsp. But no new peak arose in the HIC profiles from the hydrolysis of the IEC Asu74 fractions, indicating that if

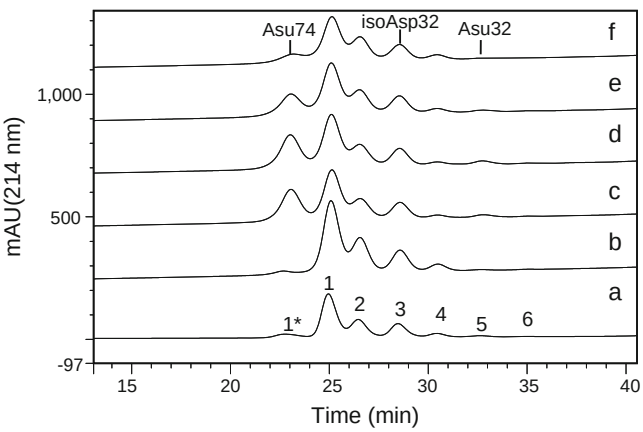

Fig. 4 Papain/HIC profiles of Fab regions of aged MAbI and IEC Asu74 fractions. Peak 1* corresponds to Asu74; nsc = non-specific clip due to papain cleavage, coelutes with peak 1*; Peak 2 is Asp32 with a free thiol group; Peak 3 corresponds to isoAsp32; and Peak 5 corresponds to Asu32. (**a**) Aged MAbI (t = 3 years @ 5°C + 23 days at 25°C); (**b**) IEC Main Peak; (**c**) Asu74-T0; (**d**) Asu74, pH 5.5; (**e**) Asu74, pH 7.0; (**f**) Asu74, pH 8.0.

isoAsp74 was present, it coeluted with the HIC peak 1 (Asp32) or with peak 3 (isoAsp32).

Since isoAsp74 in MAbI was not observed by HIC or IEC, Lys-C peptide map analysis after carboxymethylation of the IEC fractions and of MAbI stability samples was conducted. An apparent new peak in the IEC Asu74 fraction at 31 min was observed compared to the other samples (Fig. 5). An expanded view of the chromatographic region shows that the peak at 31 min is also present but at very low levels in the IEC main peak fraction and the aged MAbI sample. By LC-MS it was found that the adjacent peaks at 31 and 31.5 min have the same mass. The small peak eluting at 31 min corresponds to isoAsp74 GRITISRD$\underline{d}_{74}$SK or IsoAsp73 GRITISR$\underline{d}_{73}$DSK peptide, while the peak eluting at 31.5 min contains the Asp73-Asp74 form of the same peptide, as determined by spiking an Asp73-isoAsp74 (Fig. 5), IsoAsp73-Asp74 or Asp73-Asp74 synthetic peptide with the same sequence (data not shown). Hydrolysis of the Asu74 resulting in the formation of isoAsp/Asp is expected due to the high pH and high temperature conditions during peptide mapping, and hence Asu74 is not detected in the Lys-C map. In this case, the hydrolyzed Asu74 fraction resulted in 13% isoAsp74 and 87% Asp74.

After determining the elution position of isoAsp74 in the Lys-C peptide maps, isoAsp74 in several MAbI stability samples was quantified by Lys-C peptide mapping. Very little formation of isoAsp74 was observed even in highly degraded samples (stored up to 6 years at 2–8°C). The Lys-C maps were also used to quantify isoAsp32 in the above samples. A summary of the amounts of isoAsp (quantified by Lys-C maps) and Asu (quantified by HIC, since Asu gets completely hydrolyzed in the Lys-C maps) at both Asp32 and Asp74 in stability samples is shown in Fig. 6. A good correlation was observed for the quantification of isoAsp32 using the HIC and the Lys-C method (data not shown). As shown in Fig. 6, it is clear that Asp32 undergoes a typical isomerization reaction and produces Asu32 and isoAsp32/Asp32. However, the Asp74 isomerization reaction led to the generation of Asu74 and very little amount of isoAsp74, indicating that there is a significant difference in the hydrolysis step of the isomerization reaction between Asp32 and Asp74.

Isomerization of Model Peptides

To further study the isomerization mechanism at Asp74, the synthetic peptide GRITISRDDSK with the same sequence as the corresponding MAbI Lys-C Asp74 peptide was incubated at 25°C and 40°C for 5 weeks, under similar buffer conditions. The stability data of the GRITISRDDSK peptide show typical isomerization reaction profiles (Figs. 7 and 8), as determined by RP-HPLC. Similarly, a synthetic peptide with the sequence ISRDDSK was also put on stability and showed similar Asu/isoAsp formation rates (data not shown) as the other synthetic peptide, GRITISRDDSK. The data from the synthetic peptide show a steady state concentration of Asu and an increase in the isoAsp concentration over time as expected (17). This differs from the isomerization mechanism of Asp74 in MAbI, where we observed very little formation of isoAsp and higher accumulation of Asu (Figs. 9 and 10). This indicates that the primary sequence is not the governing factor for the observed isomerization reactions. Mechanistic and kinetic differences in the formation of Asu/isoAsp in simple peptide models *versus* proteins are not uncommon and are attributable to the differences of higher

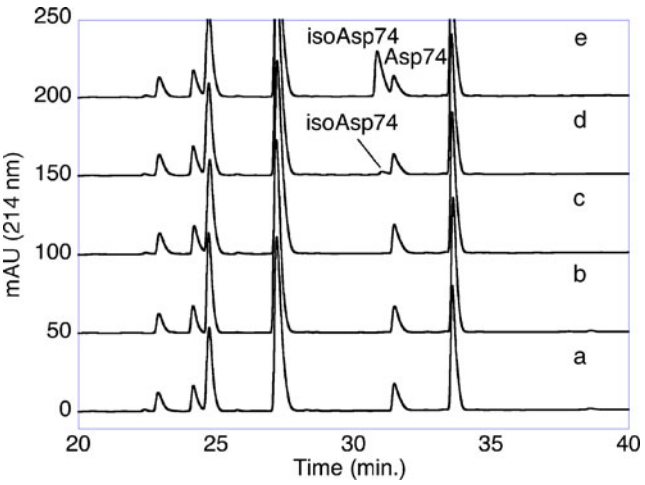

Fig. 5 Expanded view of the Lys-C maps of IEC fractions of MAbI. (**a**) MAbI, (**b**) aged MAbI (t = 3 years @ 5°C + 23 days at 25°C), (**c**) IEC main peak fraction, (**d**) Asu74-T0 fraction, E = Asu74-T0 fraction + spiked isoAsp74 peptide.

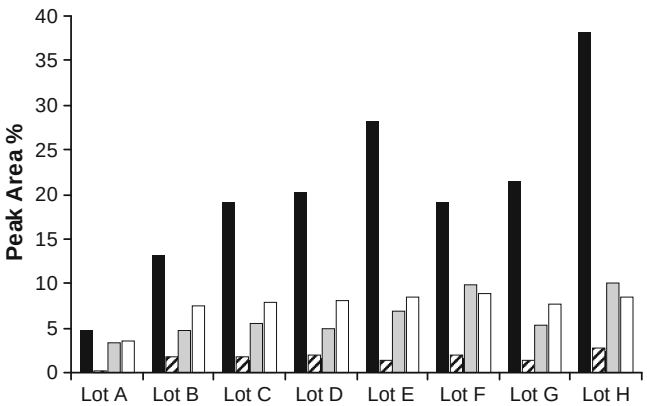

Fig. 6 Summary of the amounts of IsoAsp and Asu in MAbI samples after storage at different temperatures. Lot A is sample control, Lot B, C, D and E were stored at 5°C for 2, 3, 4.5 and 6 years, respectively. Lot F, G and H were first stored at 5°C for 2, 3 and 2 years, respectively, and then stored at 25°C for 37, 23, and 211 days, respectively. IsoAsp 32 (black) and isoAsp74 (stripes) were determined from integration of Lys-C maps, while Asu32 (light grey) and Asu74 (white) amounts were obtained from IEC.

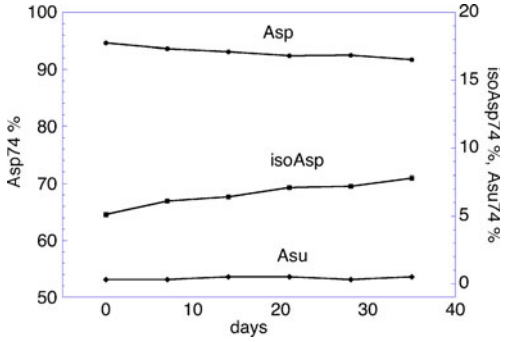

Fig. 7 Isomerization reaction of Asp74 in the LysC peptide GRI-TISRDDSK at 25°C, pH 6.0.

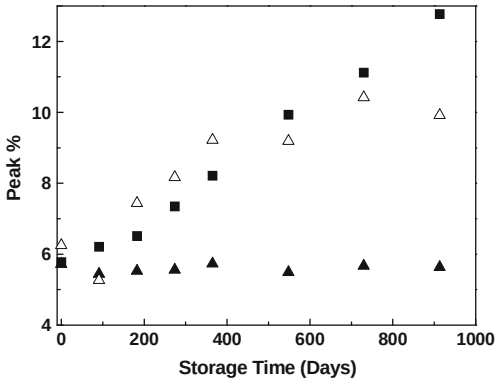

Fig. 9 Summary of HIC and IEC results for MAbI at pH 6.0 after storage at 5° C for 2.5 years. The percentage of peaks shown in figure include the IEC basic peak 1 (Asu32, ▲), basic peak 2 (Asu74, Δ) and HIC peak 3 (isoAsp32, ■).

ordered structures (17), including the secondary structure (19,20) found in MAbs and peptides.

Previous studies showed that the lack of detectable isoAsp in several proteins can be due to analytical constraints or conformational constraints (6). Another hypothetical pathway that has been proposed for the exclusive formation of reversible cyclization reaction (Asp ↔ Asu) is the formation of an isoimide instead of the more common succinimide (Scheme 2) (21). The hydrolysis of isoimide exclusively forms only aspartic acid (21). In contrast, hydrolysis of the succinimide intermediate leads to the formation of either isoAsp or Asp (typically in a 3:1 ratio) due to orientation of the hydrolytic attack (21,22). Therefore, the trace level of isoAsp74 and high level of cyclic imide form observed in this MAb could possibly be explained by the conformation constraints of succinimide and probably rules out any isoimide formation.

Analysis of Local Structure by X-ray Crystallography of MAbI

X-ray crystallography of the Fab fragments of MAbI was reported earlier (17). The solvent accessibility parameters were determined for relevant residues (−ISRD$_{73}$D$_{74}$SK-) and for Asp32 on the CDRI region of MAbI as described earlier (17). Based on the solvent accessibility data shown in Table 2, Asp74 is relatively more exposed than its neighboring Asp73. However, both aspartic acid residues are considerably less exposed to solvent than Asp32, as would be expected for an Asp residue that is in the CDR region of a MAb. From the x-ray crystal coordinates and the phi (ϕ)-psi (ψ) angles, it can be viewed (25) that Asp73 of MAbI resides in a β-helix, whereas Asp74 falls in a loop with a loosely ordered structure (26) (Fig. 11, Table 2). Xie *et al.* have shown that deamidation reaction of Asn in a random coil that is also a loosely ordered structure is significantly faster than Asn in a β-turn (27). Formation of isoAsp in the deamidation reaction of Asn proceeds via a similar Asu intermediate as the isomerization reaction. Hence, it is expected that the higher order structure of protein will have similar effect on the isomerization reaction as those observed for the deamidation reaction.

pKa values were determined using PROPKA (28,29) utilizing the known single crystal coordinates for MAbI (17)

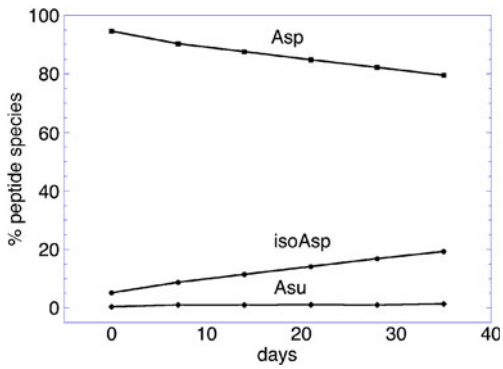

Fig. 8 Isomerization reaction of Asp74 in the LysC peptide GRI-TISRDDSK at 40°C, pH 6.0.

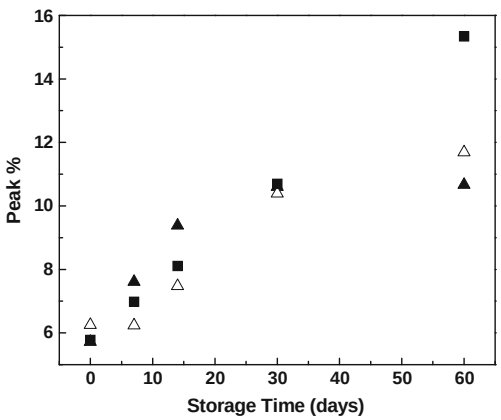

Fig. 10 Summary of HIC and IEC results for a MAbI at pH 6.0 after storage at 25°C for 60 days. The percentage of peaks shown in figure includes the IEC basic peak 1 (Asu32, ▲), basic peak 2 (Asu74, Δ) and HIC peak 3 (isoAsp32, ■).

Scheme 2 Potential pathway of Asp isomerization leading to isoimide formation in proteins and peptides (21).

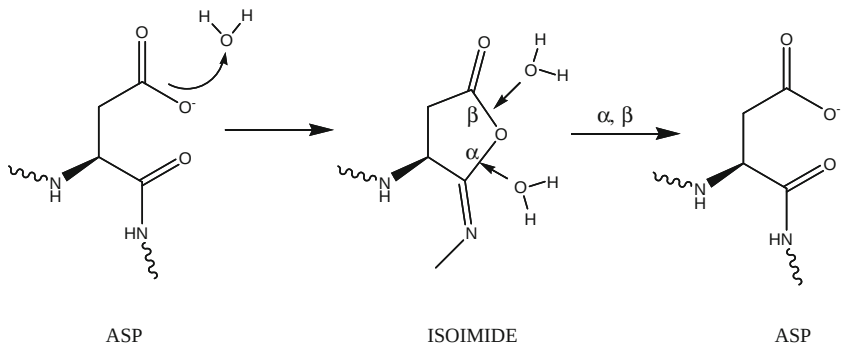

and are shown in Table 2. The pKa analysis shows that Asp73 has a pKa around 2.71, whereas Asp74 was found to have a pKa of 3.73, and L-Asp side chain pKa was predicted to be 3.80 (28,29). The pKa values of the side chain carboxylic acid on the neighboring Asp residues were considered to play a role in the isomerization reaction. The ionization of one Asp derivative would influence the pKa of the other and could possibly explain the comparative reactivity of the aspartates towards the isomerization reaction. The aspartic acid side chain can exist either as the carboxylate anion ($-COO^-$) or the protonated form ($-COOH$), of which the latter is more reactive to isomerization based on the mechanism established by Geiger and Clarke (22). Additionally, it has been reported that the side chain which predominantly exists as carboxylate anion renders the carbonyl center less prone to a nucleophilic attack by the backbone amide nitrogen and hence has a lower tendency to form an Asu or isoAsp (16).

The B-values can be used as indicators of the conformational flexibility of the amino acid side chains. B-values for some relevant atoms on MAbI were determined from the X-ray crystal structure data and the atomic resolution parameters (Table 2). As seen in Table 2, the B-values indicate that the flexibility of the β-carbon of Asp73 and Asp74 are similar, but less flexible than Asp32. The increase of side chain flexibility would allow the side chain to orient at appropriate conformation for the isomerization reaction to take place (30).

Although the structural resolution of this particular MAb Fab is low (resolution of 3.0 A°) (17), comparison of B values and solvent accessibility made within this MAb has provided some useful information. Based on previous literature reports on Asn deamidation reaction in β-turn structures *versus* a random coil (27), the relative pKa of Asp73 *versus* Asp74, the solvent accessibility data of Asp74 *versus* Asp73, and mechanism of Asp isomerization published earlier (16,22), it appears more likely that Asp74 in MAbI can undergo the succinimide formation when compared to its neighboring Asp73. Further hydrolysis of the succinimide to the isoAsp may be restricted due to limited solvent accessibility.

Degradation Profiles of Asp isomerization Reaction

The stability of Asp isomerization reaction for MAbI was studied at 5 and 25°C. The major isomerization degradation products, isoAsp32, Asu32 and Asu74 were monitored by HIC and IEC methods. As shown in Figs. 9 and 10,

Table 2 Solvent Accessibility Parameters and B-values of the β-carbon of Relevant Aspartic Acid Residues in MAbI

Residue	Solvent accessibility parameter (%)[1]	ϕ	ψ	B-values of β carbon on Asp[1]	pKa values of Asp side chain[2]
ASP32 (CDR)	71.3	−13	50	49.8	4.23
ILE70	2.6	−152	124		
SER71	29.0	−99	154		
ARG72	26.2	−170	153		
ASP73	23.2	−153	88	42.5	2.71
ASP74	40.5	−58	−30	40.9	3.73
SER75	84.2	−68	−39		
LYS76	67.7	−87	−11		
ASN77	21.9	65	53		
THR78	7.9	−150	147		

[1] Solvent accessibility parameter and B-values (local flexibility) derived using methods described in reference 17

[2] Calculated using PROPKA (http://propka.ki.ku.dk/)

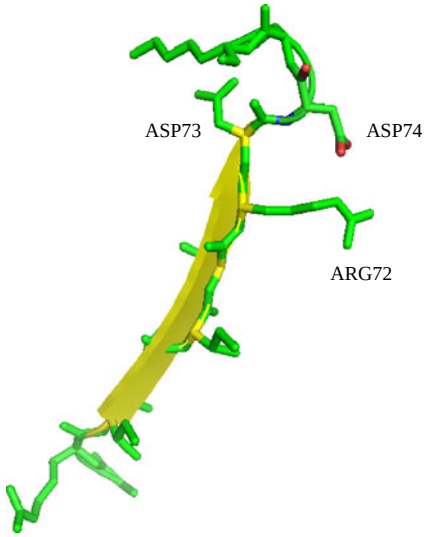

Fig. 11 Pymol view of—$RD_{73}D_{74}$—showing β-helix (yellow arrow) ending at Asp73 and loop beginning at Asp74.

isoAsp32, determined by the HIC method, showed a linear degradation profile, and Asu74, monitored by the IEC method, appears to follow a non-linear profile. Although the isomerization reaction is often described as pseudo first-order reversible reaction, the overall rate of degradation should be non-linear. The apparent linear profile for the IsoAsp formation suggests that the IsoAsp formation observed in our study is still within the initial phase, where the reversible conversion from Asu and IsoAsp to Asp is at an insignificant level. The level of Asu74 increased rapidly at the initial time points, then seems to approach a "steady state" over time at both temperatures. There is no significant increase of IsoAsp74 over time. The accumulation of Asu74 form in MAbI was different from that observed in the model peptide used in this study (Fig. 7, Table 3). For full length MAbI, there is approximately 4% increase of Asu74 and no formation of IsoAsp74 over 30 days at 25°C. In contrast, for the model peptide, there is no increase of Asu74, while approximately 2% increase of IsoAsp under the same condition was observed. Previously (17), we have observed faster isomerization reactions for the full-length antibody (MAbI) compared to its peptide model (VDYDG). A Tyr residue in H-bonding distance to Asp32 was attributed to be the likely cause of the increased reactivity by acting as the H-bond donor, especially under conditions where the pH is greater than the pKa of Asp (i.e. pH>4). In the x-ray structure, we find that Arg-72 is within H-bonding distance (2.7 A^o) to Asp74 and may contribute to the faster reactivity of the isomerization reaction of Asp74 in the full-length antibody, as compared to its peptide models. However, mechanistic details of the catalytic effect of different H-bond donors and local environment on Asp reactivity were not undertaken in this study. The apparent non-linear formation of Asu74 in the full-length antibody may be related to the reversible conversion of Asu to Asp. Similar non-linear formation of Asu32 at 25°C was also observed in the same antibody (Fig. 10).

Table 3 Summary of Degradation Profile of Isomerization Products

Isomerization products	MAb	Model peptide[1]
IsoAsp32	Linear	Linear
IsoAsp74	No changes	Linear
Asu32 at 5°C	No changes	NA
Asu74 at 5°C	Non-linear	NA
Asu32 at 25°C	Non-linear	No changes
Asu74 at 25°C	Non-linear	No changes

NA: not available

[1] Data collected at elevated temperatures

For Asp32 isomerization reaction in MAbI, a 4% increase of isoAsp32 and an additional 4% increase in Asu32 were observed over 30 days at 25°C (Fig. 10). Asu32 in MAbI appears to have different degradation profiles at different temperatures. While a significant increase of Asu32 was observed at 25°C, there was no significant increase of Asu32 at 5°C over 2 years (Table 3, Fig. 9). It appears that the initial rate of Asu32 formation is faster than the initial rate of Asu32 hydrolysis at 25°C (Fig. 10). Since the concentration of Asu32 will also govern the rate of hydrolysis, the rate of isoAsp32 formation increases as temperature and concentration of succinimide increases. Over time, the amount of Asu32 appears to reach a steady state, indicating that formation and hydrolysis reactions are at the same rate. At 5°C, the steady state of Asu32 appears to have been reached at earlier time points as a result of a small difference in the formation and hydrolysis of Asu due to lower reaction rates. Hence, no apparent change in Asu32 concentration over 2 years is observed at this temperature. The apparent differences in MAbI degradation at different temperatures also suggest that shelf life assignment should be ideally determined using real-time stability studies performed at recommended storage conditions and not by accelerated and stressed studies.

Since IsoAsp32 and Asu74 are major degradation products under normal storage conditions (2–8°C) for MAbI, the kinetics of the isomerization reaction of the major variants should be evaluated carefully to ensure an appropriate control strategy and assignment of product shelf life. The apparent differences in the isomerization profile and rates between the two aspartates (Asp32 *versus* Asp74) suggest that the higher order structure of MAbI plays an important role in the isomerization reaction.

ACKNOWLEDGMENTS & DISCLOSURES

The authors would like to thank Charles Eigenbrot for insights into the X-ray structure of MAbI, Oleg Borisov and Yi Yang for Mass Spectrometry analysis of model peptide variants and MAbI Lys-C peptide maps, respectively. We would also like to thank Aditya Wakankar and Chris Yu for helpful discussions.

REFERENCES

1. Vlasak J, Ionescu R. Heterogeneity of monoclonal antibodies revealed by charge-sensitive methods. Curr Pharm Biotechnol. 2008;9:468–81.
2. Chelius D, Rehder DS, Bondarenko PV. Identification and characterization of deamidation sites in the conserved regions of human Immunoglobulin Gamma antibodies. Anal Chem. 2005; 77:6004–11.
3. Lam XM, Yang JY, Cleland JL. Antioxidants for prevention of methionine oxidation in recombinant monoclonal antibody HER2. J Pharm Sci. 1997;86:1250–5.
4. Joshi AB, Sawai M, Kearney WR, Kirsch LE. Studies on the mechanism of aspartic acid cleavage and glutamine deamidation in the acidic degradation of glucagon. J Pharm Sci. 2005;94:1912–27.
5. Perkins M, Theiler R, Lunte S, Jeschke M. Determination of the origin of charge heterogeneity in a murine monoclonal antibody. Pharm Res. 2000;17:1110–7.
6. Napper S, Prasad L, Delbaere LTJ. Structural investigation of a phosphorylation-catalyzed, isoaspartate-free, protein succinimide: crystallographic structure of post-succinimide His15Asp histidine-containing protein. Biochemistry. 2008;47:9486–96.
7. Terashima I, Koga A, Nagai H. Identification of deamidation and isomerization sites on pharmaceutical recombinant antibody using (H2O)-O-18. Anal Biochem. 2007;368:49–60.
8. Xiao G, Bondarenko PV, Jacob J, Chu GC, Chelius D. O-18 labeling method for identification and quantification of succinimide in proteins. Anal Chem. 2007;79:2714–21.
9. Cacia J, Keck R, Presta LG, Frenz J. Isomerization of an aspartic acid residue in the complementarity-determining regions of a recombinant antibody to human IgE: identification and effect on binding affinity. Biochemistry. 1996;35:1897–903.
10. Wakankar AA, Borchardt RT. Formulation considerations for proteins susceptible to asparagine deamidation and aspartate isomerization. J Pharm Sci. 2006;95:2321–36.
11. Oliyai C, Borchardt RT. Chemical pathways of peptide degradation .6. Effect of the primary sequence on the pathways of degradation of aspartyl residues in model hexapeptides. Pharm Res. 1994;11:751–8.
12. Harris RJ, Kabakoff B, Macchi FD, Shen FJ, Kwong M, Andya JD, *et al.* Identification of multiple sources of charge heterogeneity in a recombinant antibody. J Chrom B. 2001;752:233–45.
13. Xiao G, Bondarenko PV. Identification and quantification of degradations in the Asp-Asp motifs of a recombinant monoclonal antibody. J Pharm Biomed Anal. 2008;47:23–30.
14. Chu GC, Chelius D, Xiao G, Khor HK, Coulibaly S, Bondarenko PV. Accumulation of succinimide in a recombinant monoclonal antibody in mildly acidic buffers under elevated temperatures. Pharm Res. 2007;24:1145–56.
15. Brennan TV, Clarke S. Effect of adjacent histidine and cysteine residues on the spontaneous degradation of asparaginyl-containing and aspartyl-containing peptides. Int J Pept Protein Res. 1995;45:547–53.
16. Oliyai C, Borchardt RT. Chemical pathways of peptide degradation .4. Pathways, kinetics, and mechanism of degradation of an aspartyl residue in a model hexapeptide. Pharm Res. 1993;10:95–102.
17. Wakankar AA, Borchardt RT, Eigenbrot C, Shia S, Wang YJ, Shire SJ, *et al.* Aspartate isomerization in the complementarity-determining regions of two closely related monoclonal antibodies. Biochemistry. 2007;46:1534–44.
18. Harris RJ, Chin ET, Macchi FD, Keck RG, Shyong B-J, Ling VT, Cordoba AJ, Marian M, Sinclair D, Battersby JE, Jones AJS. Analytical characterization of monoclonal antibodies: linking structure to function. Current trends in monoclonal antibody development and manufacturing (Ed Steve J Shire *et al*) 2010;193–205.
19. Sinha S, Zhang L, Duan SF, Williams TD, Vlasak J, Ionescu R, *et al.* Effect of protein structure on deamidation rate in the Fc fragment of an IgG1 monoclonal antibody. Protein Sci. 2009; 18:1573–84.
20. Xie M, Schowen RL. Secondary structure and protein deamidation. J Pharm Sci. 1999;88:8–13.
21. Athmer L, Kindrachuk J, Georges F, Napper S. The influence of protein structure on the products emerging from succinimide hydrolysis. J Biol Chem. 2002;277:30502–7.
22. Geiger T, Clarke S. Deamidation, isomerization, and racemization at asparaginyl and aspartyl residues in peptides - succinimide-linked reactions that contribute to protein-degradation. J Biol Chem. 1987;262:785–94.
23. Ionescu R, Vlasak J. Kinetics of chemical degradation in monoclonal antibodies: relationship between rates at the molecular and peptide levels. Anal Chem. 2010;82:3198–206.
24. Capasso S, Di Cerbo P. Kinetic and thermodynamic control of the relative yield of the deamidation of asparagine and isomerization of aspartic acid residues. J Pept Res. 2000;56:382–7.
25. DeLano WL. The PyMOL molecular graphics system, DeLano Scientific, Palo Alto, CA, USA. http://www.pymol.org.
26. Ramachandran GN, Sasisekharan V. Conformation of polypeptides and proteins. Adv Protein Chem. 1968;23:283–438.
27. Xie M, Aube J, Borchardt RT, Morton M, Topp EM, Vander Velde D, *et al.* Reactivity toward deamidation of asparagine residues in beta-turn structures. J Pept Res. 2000;56:165–71.
28. Li H, Robertson AD, Jensen JH. Very fast empirical prediction and interpretation of protein pKa values. Proteins. 2005;61:704–21.
29. Bas DC, Rogers DM, Jensen JH. Very fast prediction and rationalization of pKa values for protein-ligand complexes. Proteins. 2008;73:765–83.
30. Paranandi MV, Guzzetta AW, Hancock WS, Aswad DW. Deamidation and isoaspartate formation during *in vitro* aging of recombinant tissue plasminogen activator. J Biol Chem. 1994; 269:243–53.